

FULL PAPER

Open Access



Amplitude enhancement of short period GPS-TEC oscillations over rainfall area

Toshihiko Iyemori^{1*} , Akiyasu Yamada¹, Tadashi Aoyama², Kornyanat Hozumi³, Yoshihiro Yokoyama⁴, Yoko Odagi¹, Yasuharu Sano⁵, Vijak Pangsapa⁶, Thanawat Jarupongsakul⁶, Akinori Saito¹ and Masato Iguchi⁷

Abstract

Correlation between rainfall and short period GPS-TEC (total electron content) variations are investigated by using the precipitation data obtained on the ground and estimated from satellite observations (JAXA/GSMaP) as a proxy of lower atmospheric wave activity. The GPS-TEC data obtained at a tropical station, PHIM, in Phimai, Thailand, for 2014–2020, and the data obtained at a mid-latitude station, NAKG, in Tokara Nakanoshima Island, Japan, for 2017–2019, are examined. A statistical analysis of MEM (maximum entropy method) power spectral density (PSD) in the period range from 50 to 1200 s over PHIM clearly shows an enhancement in the cases of rainfall from that in no-rainfall cases, in particular, on the dusk side. The enhancement is observed both acoustic wave periods less than 5–6 min and internal gravity wave periods more than 10 min. The enhancement after sunset could be an effect of strong rainfall more frequent on the dusk side than that in other local time, or it could suggest the importance of ionospheric electron density profile change for the TEC variation. On the other hand, the PSD does not show such clear enhancement over NAKG on the dusk side, although it shows a small enhancement on both dayside and night-side. A clear PSD bulge near the main vertical acoustic resonance periods, i.e., around 275 s, appears in the average PSD profile of the TEC at PHIM, which suggests that the resonance effect contribute to some extent the PSD enhancement under rainy condition. An event analysis also suggests the contribution of acoustic resonance to the enhancement of the short period TEC variation. A complicated spatial distribution of TEC oscillation over a rainfall area around PHIM, where the TEC oscillations with various periods co-exist, is presented.

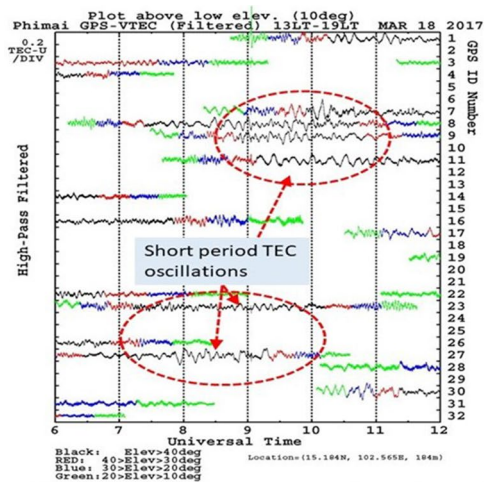
Keywords: GPS-TEC variation, Acoustic waves, Rainfall, GSMaP, Vertical acoustic resonance, Vertical coupling, Tropical squall

*Correspondence: iyemori.toshihiko.7w@kyoto-u.jp

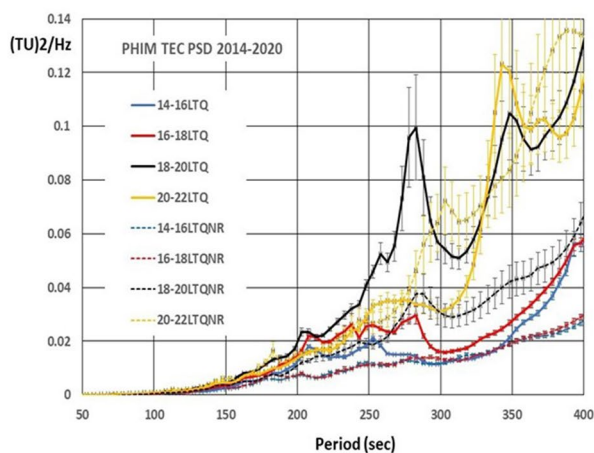
¹ Graduate School of Science, Kyoto University, Kita-shirakawa Oiwake-cho, Sakyo-ku, Kyoto 606-8502, Japan

Full list of author information is available at the end of the article

Graphical Abstract



High-pass filtered GPS-TEC data (V-TEC) observed at Phimai station (PHIM). After a strong rainfall, short period TEC variations are observed. The color of the traces indicates the elevation angle of the GPS satellites



PSDs for the LT ranges of every 2 hours from 14LT to 22LT. The solid lines with error bars indicate the PSD under the rainfall condition and the broken lines indicate the PSD under almost no-rainfall. Two lines with the same color belong to the same LT zone.

Introduction

Acoustic waves with a period shorter than about 5 or 6 min generated in lower atmosphere can propagate upward, and the waves with periods shorter than the cut-off period reach the ionosphere and causes electron density oscillations and electric currents (e.g., Shinagawa et al. 2007; Zettergren and Snively 2015). Such effects of lower atmospheric waves have been observed after huge earthquakes, typhoons, hurricanes, etc., by GPS-TEC observations, satellite observations and ground-based geomagnetic and micro-barometric observations when the waves are intensified by the vertical acoustic resonance (e.g., Calais and Minster, 1995; Kanamori et al., 1994; Heki and Ping 2005; Iyemori et al. 2005; Choosakul et al. 2009; Saito et al. 2011; Nishioka et al. 2013).

On the other hand, with precise magnetic field measurements by the satellites such as the CHAMP or the Swarm, small-scale magnetic fluctuations are commonly observed in low- and mid-latitude ionospheric F-region mainly on the dayside, and it has been presumed that they are generated by the waves from lower atmosphere because of their geographical dependence and seasonal variations of the amplitude (e.g., Nakanishi et al. 2014; Aoyama et al. 2016, 2017). The electron density also shows small-scale fluctuations on the dayside similar to the magnetic fluctuations, and their amplitude, i.e., amplitude of both magnetic and electron fluctuations, increases over the rainfall area (Iyemori et al. 2022).

In this paper, first, we present some examples of correlation between the weather parameters observed at a tropical station and the GPS-TEC oscillations over the station. Then we statistically analyze the correlation of rainfall with the power spectral density of the GPS-TEC oscillations over the two stations, one in the tropical zone and another in the mid-latitude. The precipitation data estimated by the JAXA/GSMaP are used as a proxy of lower atmospheric wave activity.

Data

The data from two GPS stations, PHIM at Phimai, Thailand (15.184 N, 102.563 E) and NAKG at Tokara Nakanoshima Island, Japan (29.841 N, 129.877 E) are analyzed. At both Phimai and Nakanoshima Is., weather parameters such as temperature, wind velocity, pressure, humidity, rainfall are observed by a weather station, Vaisalla WXT520, and data are recorded with one second cadence although the actual resolution for rainfall is 10 s. Geomagnetic field and micro-barometric data are also recorded with one second resolution.

The GPS receivers used at Phimai are a TPS E_GGD until February 4, 2017, and a TR_G2T after March 13, 2017, and the data are recorded with 1-s cadence. The GPS receiver at Nakanoshima Is. is Leica GRX1200+GNSS, and recorded with 1 s cadence from July 25, 2017 to August 5, 2018, and with 15 s cadence after August 26, 2018. The data obtained at these two

stations are not continuous because they are un-manned stations and weather conditions are rather severe by lightnings, typhoons, etc. In this paper, the PHIM TEC data from March 1, 2014 to December 31, 2020 (total 1764 days) and the NAKG TEC data from July 25, 2017 to July 20, 2019 (total 645 days) are analyzed. The raw data files are converted to Rinex format (Ver. 2.10) and derived the slant TEC values with the method described, for example, Heki et al. (2010). The vertical TEC (V-TEC) values converted from slant TEC (S-TEC) are used in this paper.

The rainfall intensity as a proxy of lower atmospheric disturbance, we use the rainfall data obtained by the WXT520 weather station at the two GPS stations and the JAXA/GSMaP estimation in the surrounding area of the two stations. The JAXA/GSMaP provides an estimation of global hourly rainfall (<https://sharaku.eorc.jaxa.jp/GSMaP/index.htm>). The GSMaP uses Dual-frequency Precipitation Radar (DPR) onboard Global Precipitation Measurement (GPM) core satellites, other GPM constellation satellites, and Geostationary satellites (<https://sharaku.eorc.jaxa.jp/GSMaP/guide.html>). The hourly rainfall data are used in this paper, and they are available since March 2014 with a spatial resolution of $0.1^\circ \times 0.1^\circ$ in geodetic latitude and longitude.

Figure 1 presents an example of weather parameters observed on March 18, 2017 when we had a severe weather change at Phimai area. A strong wind and precipitation started around 07:30UT (Universal time). The local time (LT) is around 14:30LT (LT=UT+7). The maximum strength of the precipitation was near 50 mm/h, and other parameters also changed suddenly at the start of the precipitation. This is, so-called, a tropical squall where a sudden increase of wind speed more than 8 m/s is observed, and it often accompanies a strong precipitation. The pressure shows short period oscillations shortly before the start of precipitation (bottom panel).

Figure 2 shows the GPS-TEC variations for 06–12UT (13–19LT) on the same day with Fig. 1. Each trace shows the GPS-TEC data high-pass filtered by a Gauss filter with standard deviation $\sigma=120$ s. The numbers on the right of the panel are the GPS satellite ID (PRN). The color of each trace indicates the elevation angle (EL), i.e., green; $EL < 20^\circ$, blue; $20^\circ < EL < 30^\circ$, red; $30^\circ < EL < 40^\circ$, black; $EL > 40^\circ$. The multi-pass effects are seen on the trace during lower elevation angle as the oscillations with various periods that probably depend on the apparent inclination angle of the satellite orbit. Because such oscillations sometimes appear even around 40° , when we statistically analyze the power spectral density (PSD) of the TEC data, we use the data with EL greater than 50° in this paper. In this event on March 18, 2017, we see short period fluctuations encircled by two red broken lines after around 08UT.

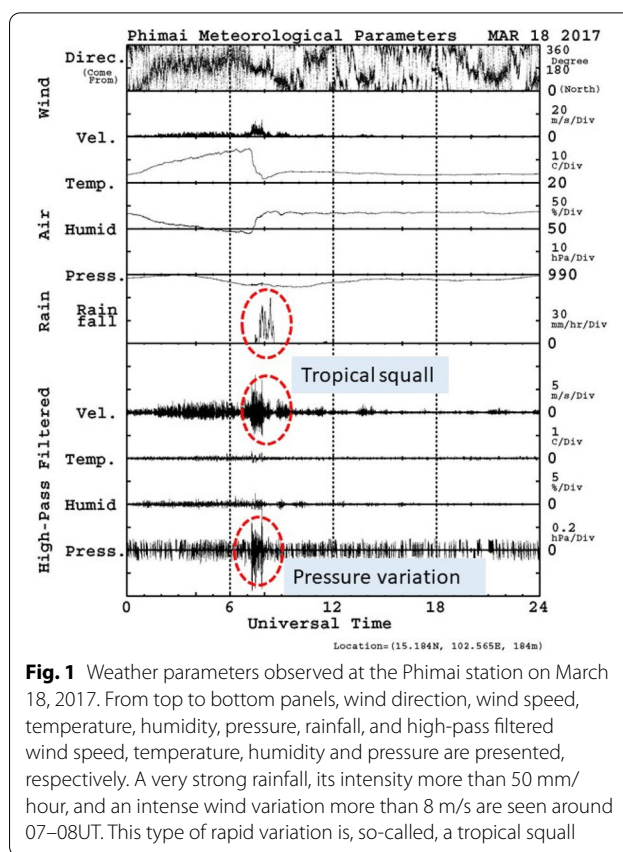
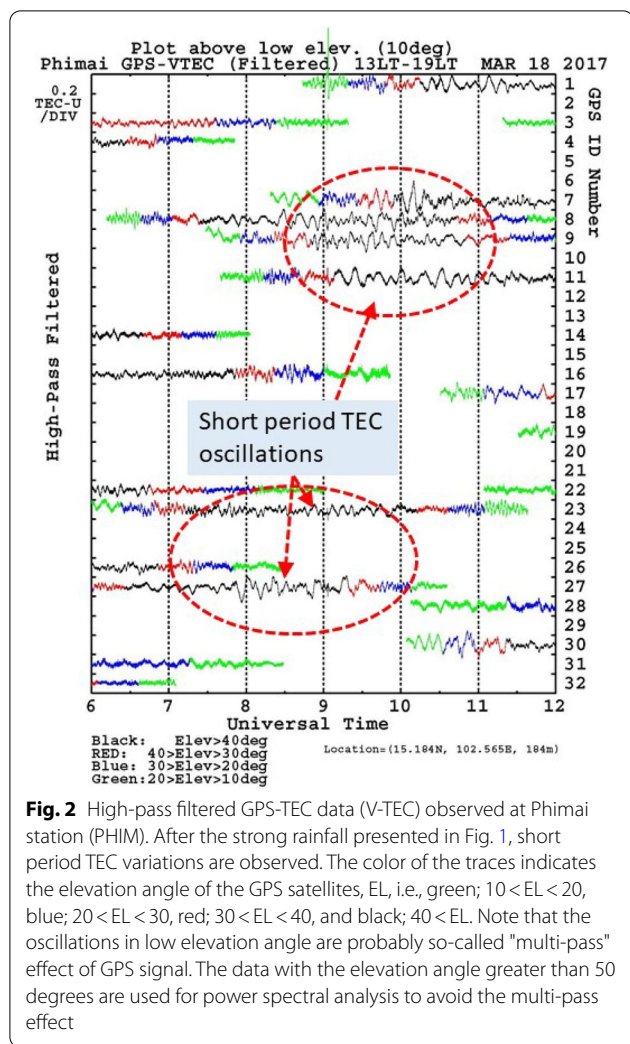


Fig. 1 Weather parameters observed at the Phimai station on March 18, 2017. From top to bottom panels, wind direction, wind speed, temperature, humidity, pressure, rainfall, and high-pass filtered wind speed, temperature, humidity and pressure are presented, respectively. A very strong rainfall, its intensity more than 50 mm/hour, and an intense wind variation more than 8 m/s are seen around 07–08UT. This type of rapid variation is, so-called, a tropical squall

Figure 3 shows the power spectral density of the GPS-TEC data calculated by a MEM (maximum entropy method) for each satellite using the data in each one hour, i.e., 3600 data points. The length of 'lag' in MEM calculation is set to be 1200, i.e., 1/3 of the data length. We calculate and plot the PSD only when the elevation angle is greater than 50° for all of the 3600 data points. The satellite ID is shown on the top of the panel with color which correspond to the color of PSD trace. Note that a tapering factor, $F = T^{1.5}$, where T is the period (s), is applied to reduce the PSD value at longer period so as to be able to present with linear scale in one panel. That is, the value is reduced at longer period. This is to see the spectral peaks clearly on the plot. In the statistical analysis, we do not use such tapering. From this figure, we see many spectral enhancements (peaks) in the period range of acoustic waves encircled by red broken line and also in the period range of internal gravity waves encircled by blue dotted lines.

To check how the MEM spectral density changes by the length of 'lag', Fig. 4 shows a comparison of two cases, lag=1200 (upper panel) and lag=900 (lower panel), respectively. As expected, although the height or sharpness of spectral peaks increases for lag=1200 case, the peak periods are the same with those for



lag = 900 case. We adopt lag = 1200 because there appears no false peak. It is said that the area size below the spectral curves, i.e., power, is nearly the same even if the height of peak changes with length of 'lag'. Although not shown in this paper, the statistical results with lag = 900 are almost the same for Figs. 8, 9, 10, 11, 12, 13 calculated with lag = 1200. The difference in the spectral height for the two cases disappears in the statistical results by averaging process.

Figures 5, 6 and 7 show another case on March 16, 2017, 2 days before the previous event. The rapid change of wind speed and strong rainfall may be categorized to a tropical squall although the amplitude of wind speed increase is slightly less than 8 m/s used in the definition of squall, i.e., it was 6.2 m/s around 07:38UT. The TEC shows similar characteristics with those in the previous event after strong precipitation.

There are many such events, however, there also many events when any precipitation is not observed at Phimai observatory probably because the area of precipitation is rather narrow or deviate from Phimai.

There would be other method than using the rainfall at a station to identify a heavy rainfall, such as using microbarometric fluctuations or using the GSMaP estimation. Before analyzing many such events in detail as a case study, in this paper, we report the results of a statistical analysis on the correlation between rainfall and the power spectral density of GPS-TEC variations to show the common existence of lower atmospheric weather effects in the upper atmosphere.

Method of analysis

We compare the average power spectral density (PSD) of the GPS-TEC variation in the cases of rainfall and that in almost no rainfall in the surrounding area of the GPS stations, PHIM or NAKG. Taking into account the condition that we use the TEC data when the elevation angle of the GPS satellite is higher than 50° and the TEC value mainly indicate the electron content in the ionospheric F-region around 300 km height, we use the rainfall data estimated by the GSMaP in 720 km × 720 km area surrounding the GPS station. We average the rainfall in the area every 1 h, and at the same time, we also record the maximum precipitation in the area.

The GPS-TEC data with 1-s cadence for PHIM and those with one second and 15 s for NAKG stations are high-pass filtered by a Gauss filter with a weighting function of Gauss distribution with $\sigma = 120$ s for the plots in the form of Figs. 2 and 6. Because the cut-off of the Gaussian-type filter is not very sharp, the signal with period longer than 10 min still remain to some extent.

We use the MEM because of its much better frequency (or period) resolution than the FFT (fast Fourier transformation) to see whether or not the vertical acoustic resonance is contributing or not. A MEM spectrum is calculated from each 1-h continuous data period with a period resolution of 1 s even for the NAKG data with 15 s cadence, i.e., from 240 data points. This is another advantage of MEM.

Because both satellites and waves are moving, we need to estimate the shift of period of TEC variation, i.e., the Doppler effect. As a simple example, we assume an acoustic wave with period of 250 s and velocity 800 m/s propagating in horizontal direction at an altitude of 300 km. It propagates about 200 km in one period. The viewing angle for 200 km length near zenith is about 37° from the ground. On the other hand, because the orbital period of the GPS satellite is about 12 h and the radius of the orbit is about 20,200 km, the viewing angle of satellite

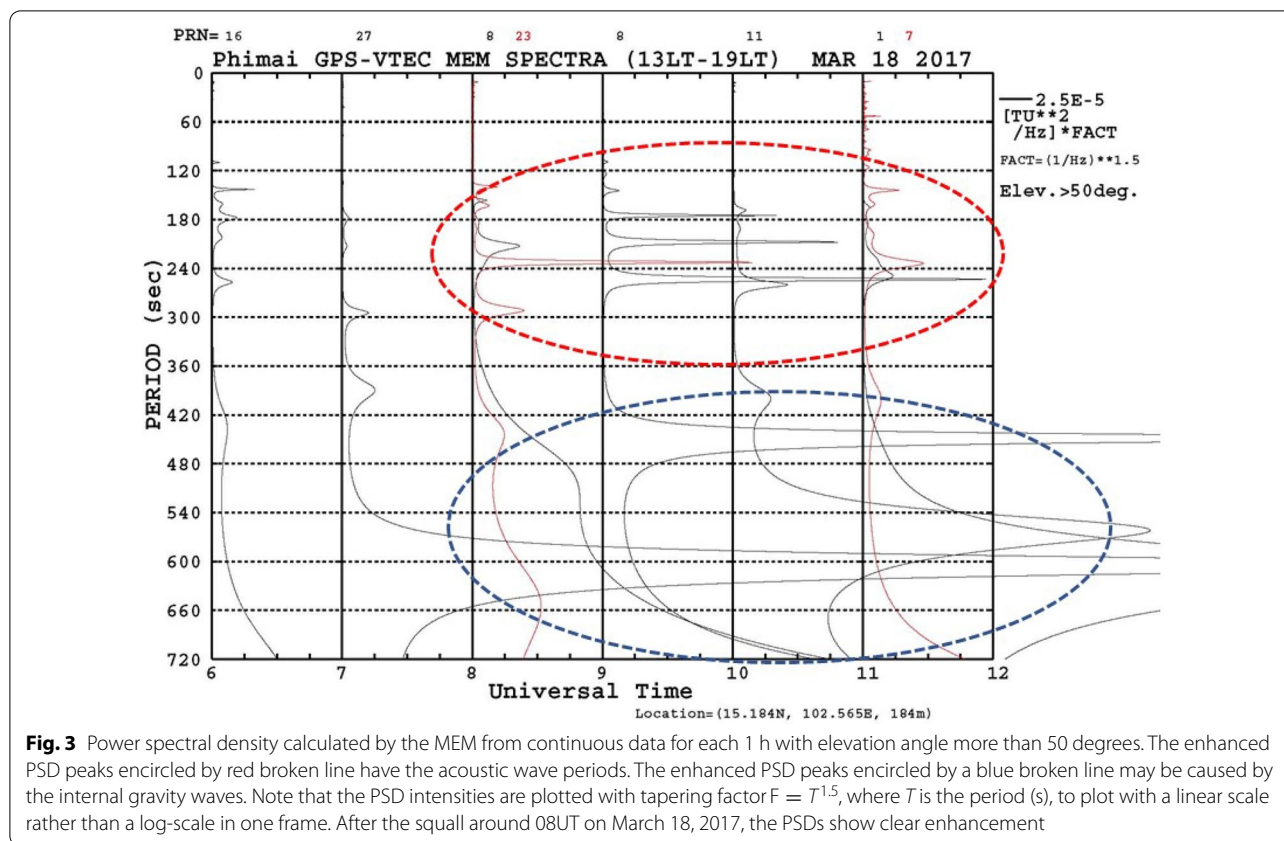


Fig. 3 Power spectral density calculated by the MEM from continuous data for each 1 h with elevation angle more than 50 degrees. The enhanced PSD peaks encircled by red broken line have the acoustic wave periods. The enhanced PSD peaks encircled by a blue broken line may be caused by the internal gravity waves. Note that the PSD intensities are plotted with tapering factor $F = T^{-1.5}$, where T is the period (s), to plot with a linear scale rather than a log-scale in one frame. After the squall around 08UT on March 18, 2017, the PSDs show clear enhancement

movement from the ground in 250 s is about 3° around the zenith. That is, the propagation speed (angular velocity) of an acoustic wave is about 12 times faster than the satellite angular velocity. Therefore, we are observing essentially the temporal variation at a slowly moving point in the sky for horizontally propagating acoustic waves. The apparent period of TEC variation would include the Doppler effect depending on the relative direction between satellite velocity and wave propagation direction. The maximum effect is about 8% of the wave period when the satellite velocity and wave propagation direction are parallel. That is, for the waves with period of 250 s, the Doppler effect is less than 20 s. For vertically propagating waves, we do not need to consider the Doppler effect because the satellite direction and wave propagation direction are orthogonal each other.

To see the correlation of rainfall to the PSD of GPS-TEC fluctuations, we compare the average PSD under the conditions when the average rainfall in 720 km × 720 km area is greater than 0.04 mm/h and when that is less than 0.002 mm/h. The reason why the threshold of no-rain condition is not zero but 0.002 mm/h is that the chance of no-rain in 720 km × 720 km is very small. Under the $K_p \leq 2$ conditions, the number of the hours for the cases

greater than 0.04 mm/h and less than 0.002 mm/h are 19,722 and 6514, respectively, at Phimai, Thailand. On the other hand, for Nakanoshima Is., we set the threshold for rainy cases as greater than 0.08 mm/h, because the amount of rainfall in the area is much more than that in Thailand as seen in Figs. 15 and 16. With this threshold, the number of the cases for Nakanoshima Is. is 4476 for rainfall and 2602 for no-rain, respectively.

Results and discussion

Figures 8 and 9 show the results of average PSDs at PHIM station for four local time zone, 08–16LT, 16–20LT, 20–04LT and 04–08LT. Note that the LT ranges are not even. The blue and red lines indicate the average PSDs in rainy (>0.04 mm/h) cases and the green and orange lines indicate those in no-rain (<0.002 mm/h) cases. The geomagnetic pulsations such as Pc5 have similar period with the TEC oscillation treated in this paper. Because the Pc5 pulsations tend to appear geomagnetically disturbed condition, we compare the PSDs under geomagnetically quiet and those under disturbed conditions by using the three hourly K_p index (see, for example, <https://www.gfz-potsdam.de/en/kp-index/>). In this paper, we adopt $K_p = 2$ as the threshold of quiet period definition. The red and

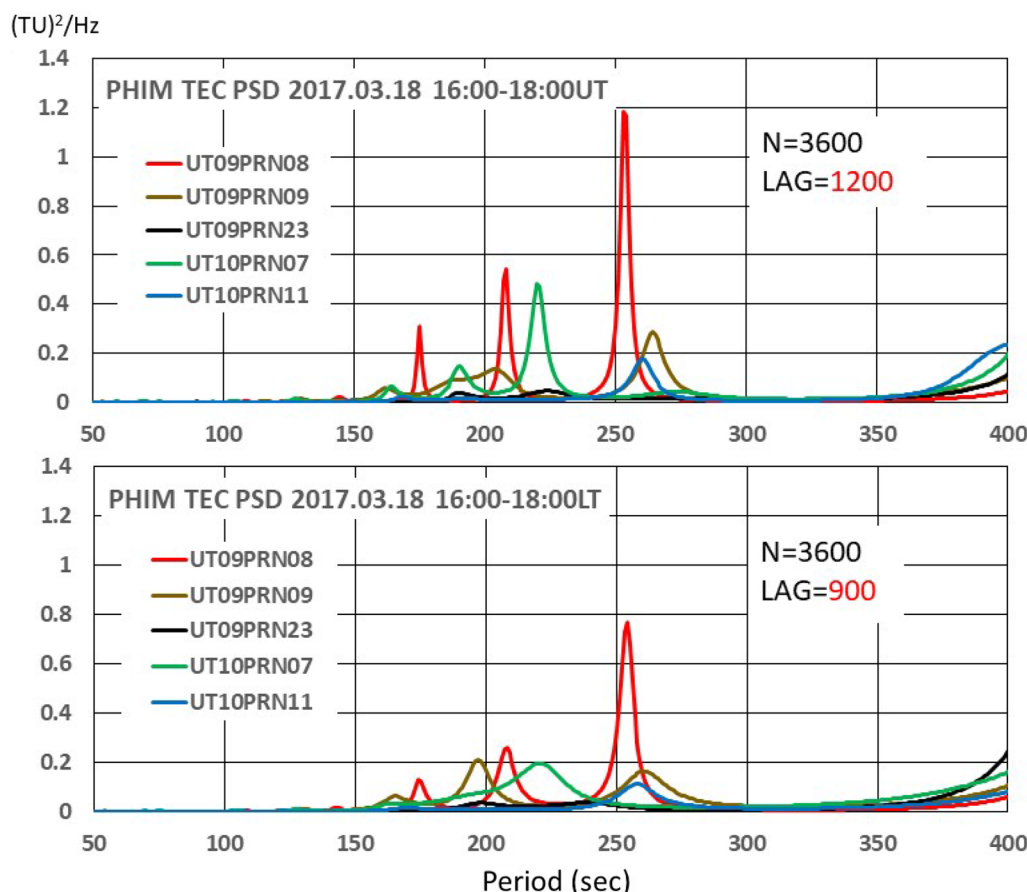


Fig. 4 A comparison of spectral density for different lag length in MEM. The upper panel shows the results for lag = 1200 and the lower panel shows those for lag = 900. These spectra correspond to some traces in Fig. 3. The UT and PRN are indicated in the panels

orange lines indicate the cases under geomagnetically quiet (i.e., $K_p \leq 2$) condition. The error bars indicate the standard error ($= \sigma/\sqrt{n}$), where σ is the standard deviation and n is the number of hours.

Figure 8 shows, in particular on the dusk side (16–20LT), the PSD in acoustic wave period clearly increases under the rainy condition. On the other hand, Fig. 9 shows that the PSD on the night-side and that on the dawn side are almost the same for the two rainfall conditions although the PSD under rainy condition is slightly larger than that under no-rain condition. The PSD under geomagnetically quiet condition, i.e., the $K_p \leq 2$, is slightly smaller than the case which include all geomagnetic condition as seen in 16–20LT case in Fig. 8. Although the geomagnetic disturbance effect is small, the results shown in Figs. 10, 11, 13 and 14 are the results under geomagnetically quiet ($K_p \leq 2$) condition.

To see the LT difference in more detail, we average the TEC PSD in every 2 h of LT. Figure 10 indicates the results for the LT ranges from 14:00LT to 22:00LT every 2 h. From this figure, we see that the effect is most clear

in 18–20LT. In 14–16LT and 16–18LT, the enhancement in rainy condition is also seen, but in the late evening, 20–22LT, such difference is not seen. We notice a common bulge of the PSD traces around a period of 275 s which is close to the fundamental mode of vertical acoustic resonance (e.g., Shinagawa et al. 2007). In Phimai area, a strong rainfall tends to occur in the evening as seen in Figs. 15 and 16, and this could cause the clear enhancement of TEC variation seen in Fig. 10.

Figure 11 shows the PSDs for wider period range which include the period of internal gravity waves. The LT ranges for this figure are the same with those of Fig. 10. We see similar LT tendency of rainfall dependence with that seen in Fig. 10. That is, the PSD enhancement in rainy condition is largest in 18–20LT even in the longer period than 10 min. Although not shown here, we do not see any clear enhancement under rainfall condition from mid-night to dawn side zones.

Figure 12 is a similar plot for NAKG station with that of Figs. 8 and 9 but in one panel. Different from the results

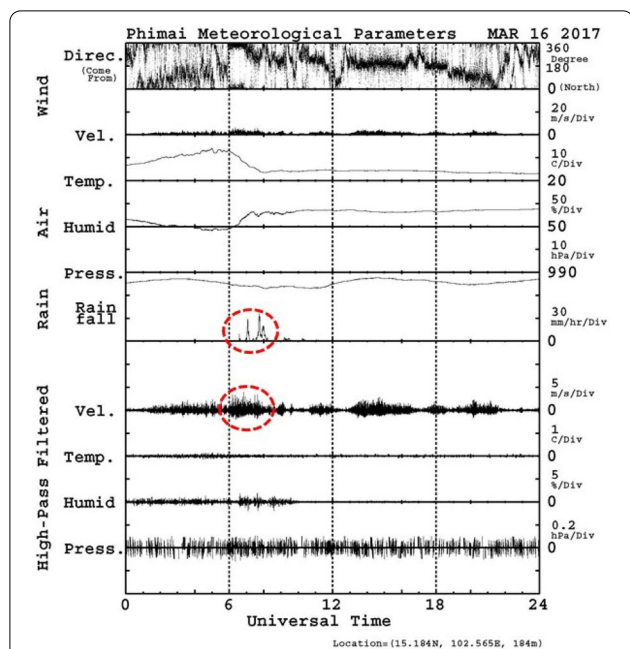


Fig. 5 Another example of strong rainfall and rapid variation of wind speed and temperature around 06–08UT on March 16, 2017

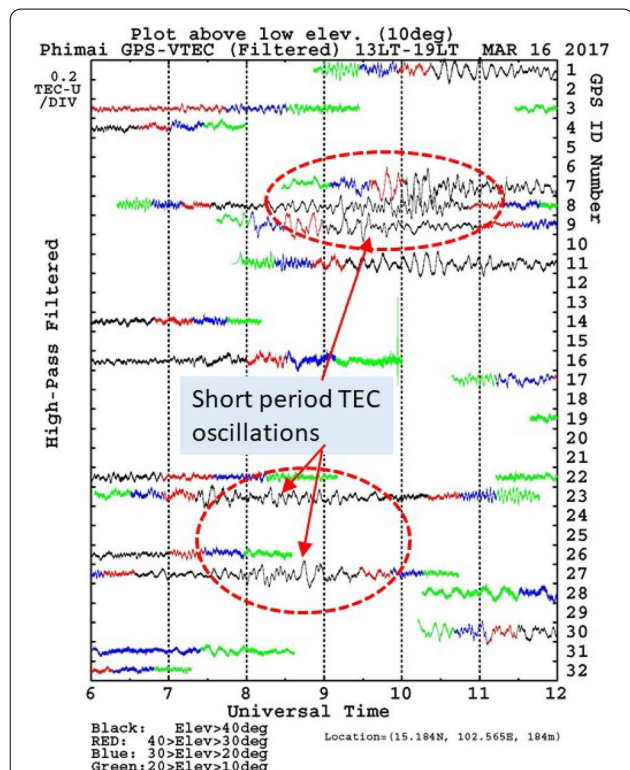


Fig. 6 TEC variation after the strong rainfall on March 16, 2017. After the rainfall around 07UT–08UT indicated in Fig. 5, short period oscillations are observed

for PHIM data, the PSD enhancement under rainfall condition is not very clear except for 20–04 LT zone.

To see which LT zone most clearly shows the correlation with rainfall, the PSD in the LT zone of every two hours are calculated, and Fig. 13 shows the results for the night-side. The difference between rainy and no-rain conditions is clearly seen in 22–24LT and 02–04LT zones.

Figure 14 is similar to Fig. 10 but for NAKG data. For longer period than 400 s, we do not see any clear PSD difference between rainy and no-rain cases except for 22–24LT (black line) zone and 02–04LT (purple line) zone.

The way of the interaction between the neutral atmospheric waves and the ionospheric plasmas may not be very different for different LT. Therefore, one possible explanation on the clear LT dependence in PHIM data could be the more frequent occurrence of strong rainfall on the dusk side than other local time zones in tropical area. Another possibility is the difference in the vertical structure of ionospheric electron density. The electron density profile change is expected to be more drastic over Phimai than mid-latitude station NAKG, because PHIM is located under the equatorial electron anomaly region. That is, the equatorial fountain effect makes a dense F-region during the daytime, however, it decreases after the sunset and the electron density gradient develops, and it is expected to be steeper than that in middle latitudes. Then the movement of plasmas by the neutral atmospheric waves could cause larger electron density variation, or the Rayleigh–Taylor type instability could be triggered.

The time scale of a tropical squall is, in general, shorter than that of the rainfall in mid-latitude, however, the strength is very strong. Such rapid and strong precipitation and wind or their sharp spatial structure could generate strong atmospheric waves.

Figure 15 presents the LT variation of average intensity (mm/h) of rainfall in 720 × 720 km area surrounding the PHIM station (upper panel) and that of the NAKG station (lower panel). Each line indicates the average for the month indicated with the same color. In PHIM area, the rainfall, i.e., the total amount of precipitation in the area, increases on the evening side except for the dry season. On the other hand, in NAKG area, the rainfall is larger on the dayside in summer (June–August) and it is almost flat in other months.

The maximum of average rainfall in the evening in PHIM area may correspond to the appearance of clear difference in the TEC PSD between rainy and no-rain conditions.

Figure 16 presents the average for 12 months. In this figure, the averaged intensity of most intense precipitation among the 0.1° × 0.1° mesh (i.e., about 4350

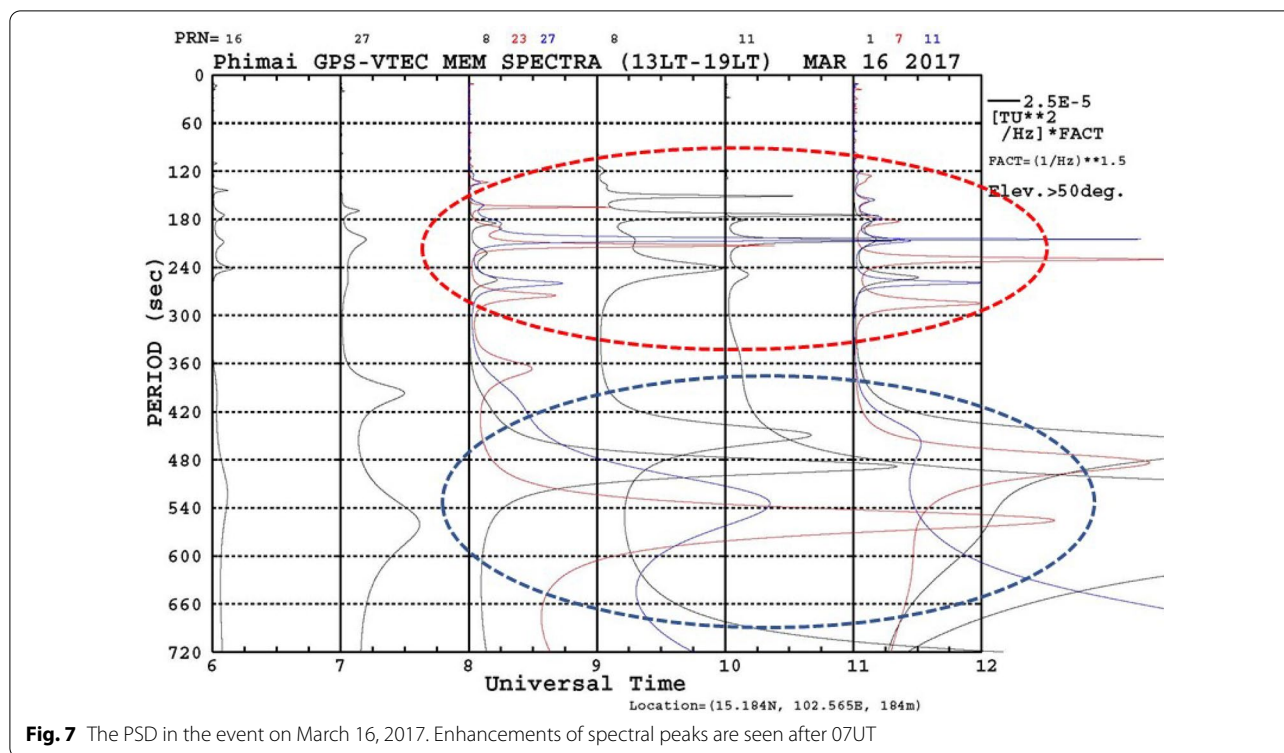


Fig. 7 The PSD in the event on March 16, 2017. Enhancements of spectral peaks are seen after 07UT

points) in 720×720 km area is also shown with dashed lines. In Phimai area, the peak of this average of most intense precipitation appears in the early afternoon (13:00–14:00LT) and the second peak appears in the late evening (21:00–22:00LT). The early afternoon peak may correspond to the occurrence of tropical squall or similar localized heavy rainfall. In the NAKG area, the simple average and the average of maximum intensity show similar LT variation. These differences of the LT variations between PHIM area and NAKG area probably comes from the difference of the type of rainfall.

In the NAKG area, Fig. 15 shows a clear enhancement of average rainfall in summer season (June, July and August) and pre-noon time zone. Figure 17 presents the TEC PSD for the summer season and other seasons. The local time zone is 10LT–12LT. As expected from the PHIM case in the evening when the average rainfall enhances, a clear enhancement of TEC PSD under rainy condition is observed. This result suggests that the amount of rainfall, i.e., strong cumulous convection in wide area is an important factor for the generation of short period TEC oscillations.

The PSDs of TEC oscillation frequently have rather sharp spectral peaks, i.e., nearly monochromatic oscillations. Figure 18a shows the meteorological parameters on April 25, 2014 at the Phimai station where a

short period wind velocity and temperature fluctuation are observed in the first half of the day. In particular, a rapid wind speed variation suddenly starts at around 10:00UT, and shortly before the variations, the TEC data from three GPS satellite, PRN=1, PRN=19 and PRN=27, show the start of large-amplitude sinusoidal waves as seen in Fig. 18b.

Their PSD is presented in Fig. 19, where sharp spectral peaks appear at the periods of 250, 215, and 180 s. These spectral peaks are shorter about 15~20 s each than the well-known three main periods of vertical acoustic resonance around ~270, ~230 and ~200 s (e.g., Shinagawa et al. 2007) reported at various occasions such as strong Earthquakes, volcanic eruptions and tornadoes. This shift of peak period could be caused by the Doppler effect discussed in 'Method of analysis' section. However, a similar set of spectral peaks is seen also in Fig. 4. The spectral peaks at 250 and 215 s of the large-amplitude TEC oscillations as observed in this event could correspond to the small spectral bulges around the periods 250 and 215 s seen in the average spectra for 14–16LT, 16–18LT and 18–20LT in Fig. 10. This could suggest an existence of slightly modified resonance in this area and these local time zones from well-known vertical acoustic resonance.

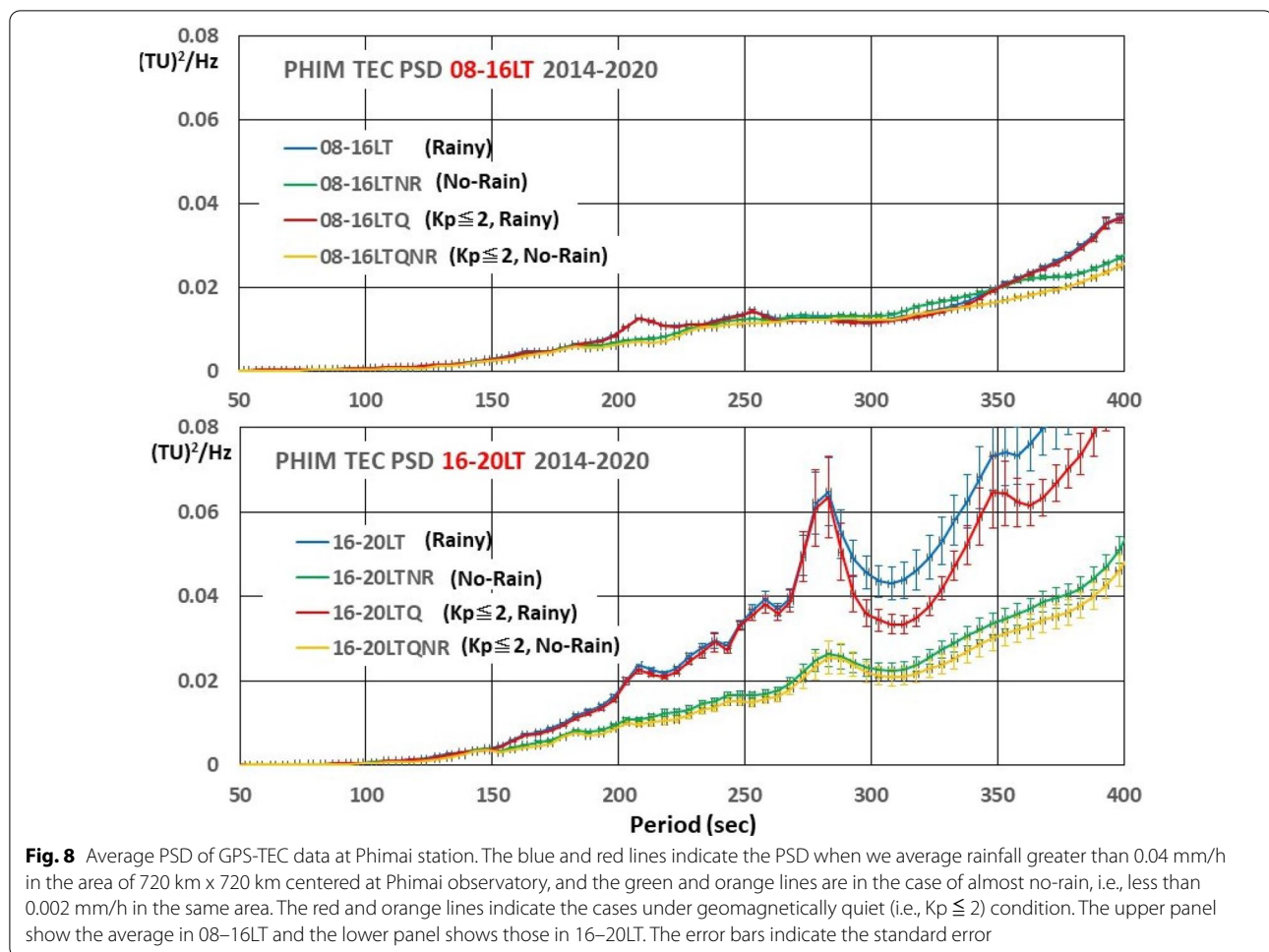


Figure 20 presents the GPS orbits and TEC variation along the orbits (left panel) and rainfall distribution estimated by the GSMaP around PHIM station (right panel) in 720 km \times 720 km area. The large-amplitude oscillations of the TEC obtained from PRN = 3, 11, 19 and 27 GPS satellites are in the north-east direction from PHIM and a strong rainfall is observed at north border of this area. The PHIM station is at the edge of another rainfall area and no strong rainfall is observed on the ground at PHIM. The strong rainfall observed at the north border could cause the large-amplitude monochromatic oscillation. On the south of PHIM station, longer period and irregular oscillations are observed. That is, various types of oscillations appear in the ionosphere over PHIM at the same time, indicating a very complicated situation over the rainfall area. To check whether or not such complicated situation is common or not, more event study is necessary.

Summary and conclusion

Correlation between rainfall and short period GPS-TEC oscillation over the two GPS stations, PHIM and NAKG, are investigated by using the MEM power spectral density of GPS-TEC data, high-time resolution ground meteorological observation and the rainfall estimation by JAXA/GSMaP. A comparison of average PSDs in rainy condition and those in almost no-rain condition shows clearly the PSD enhancement in rainy condition. However, the local time when the enhancement clearly observed is not very wide. The LT zone of PSD enhancement is mainly on the dusk side at Phimai, Thailand, and it is on the dayside and night-side at Nakanoshima Is., Japan.

Some examples indicate the amplitude enhancement of TEC fluctuations just after the tropical squall or after similar sudden change of weather condition in Phimai area. They occurred in the afternoon. On the other hand, in Phimai area, the average rainfall is larger in the evening, i.e., 18–22 LT, and the effect of rainy condition on the TEC PSD is most clear in 18–20 LT zone. The

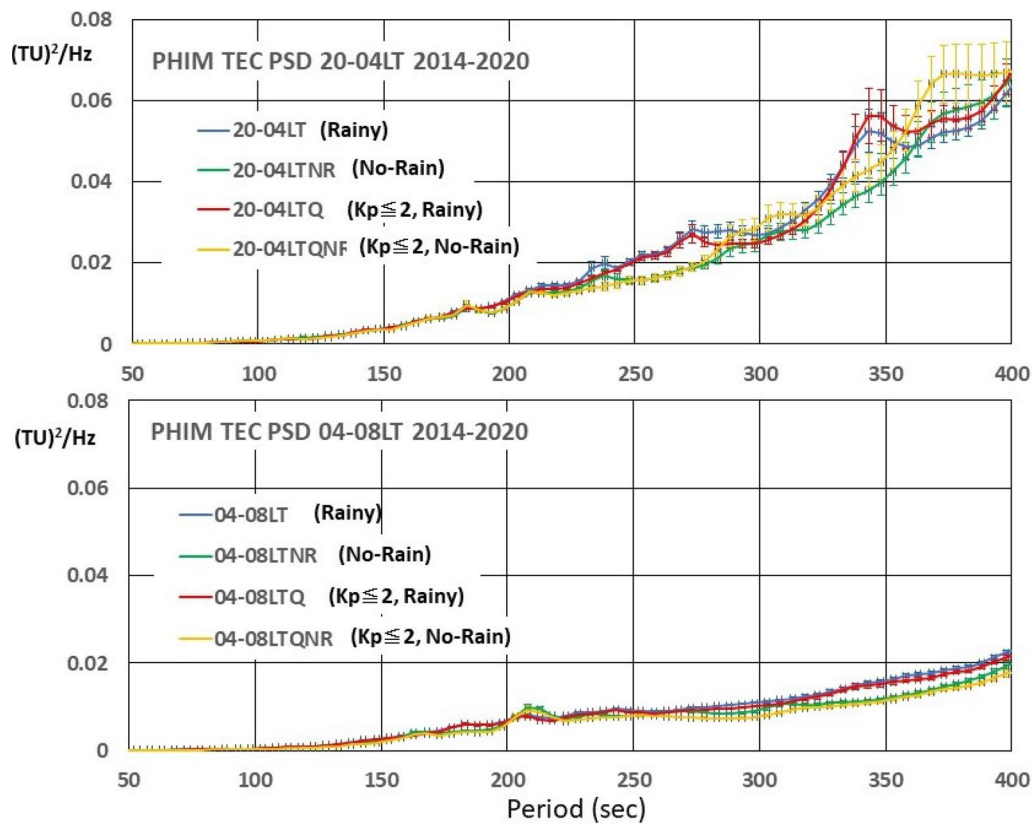


Fig. 9 Same as Fig. 8, but for 20–04LT (upper panel) and for 04–08LT (lower panel)

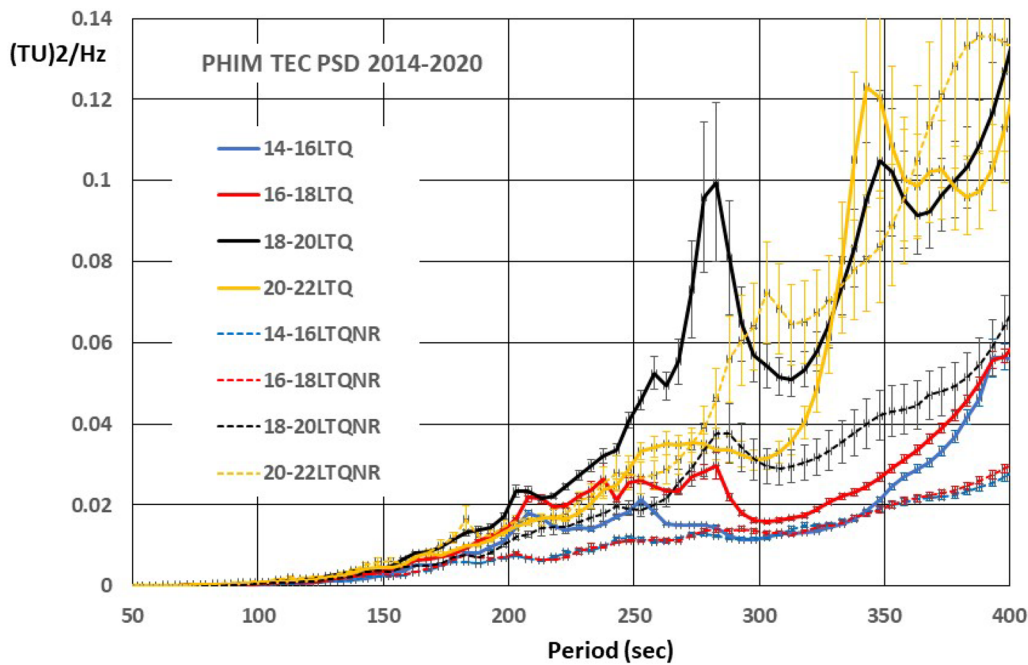


Fig. 10 PSDs for the LT ranges of every 2 h from 14 to 22LT. The solid lines indicate the PSD under the rainfall condition and the broken lines indicate the PSD under almost no-rainfall. Two lines with the same color belong to the same LT zone. The error bars indicate the standard error. The data during geomagnetically quiet period, i.e., $K_p \leq 2$, are used

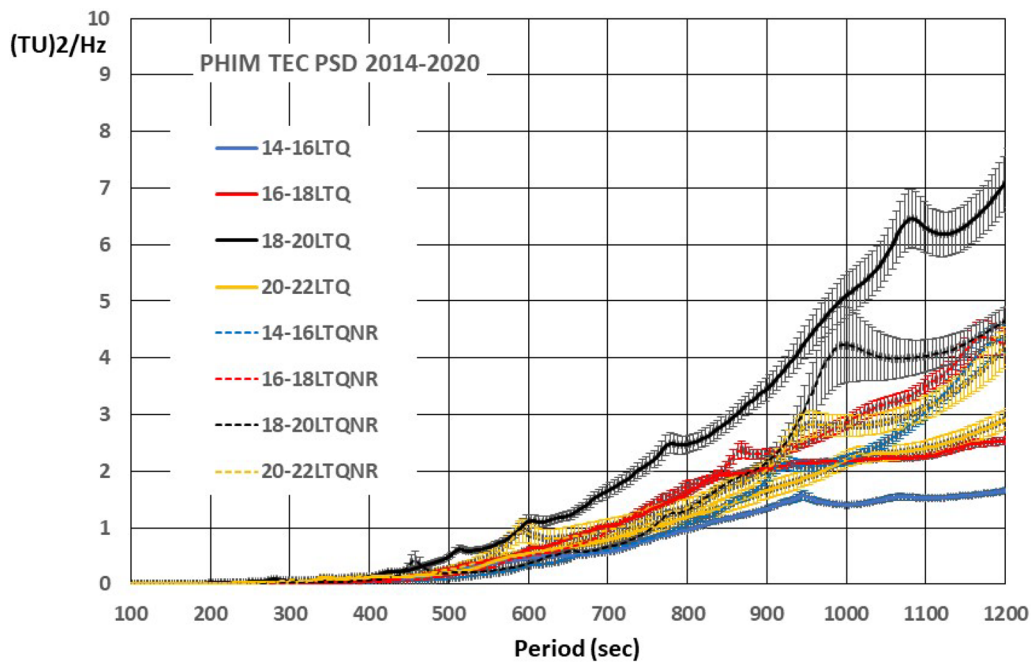


Fig. 11 The PSDs for a wide period range from 100 to 1200 s. The effect of rainfall is most clear in 18–20LT which is similar to the short period range presented in Fig. 10

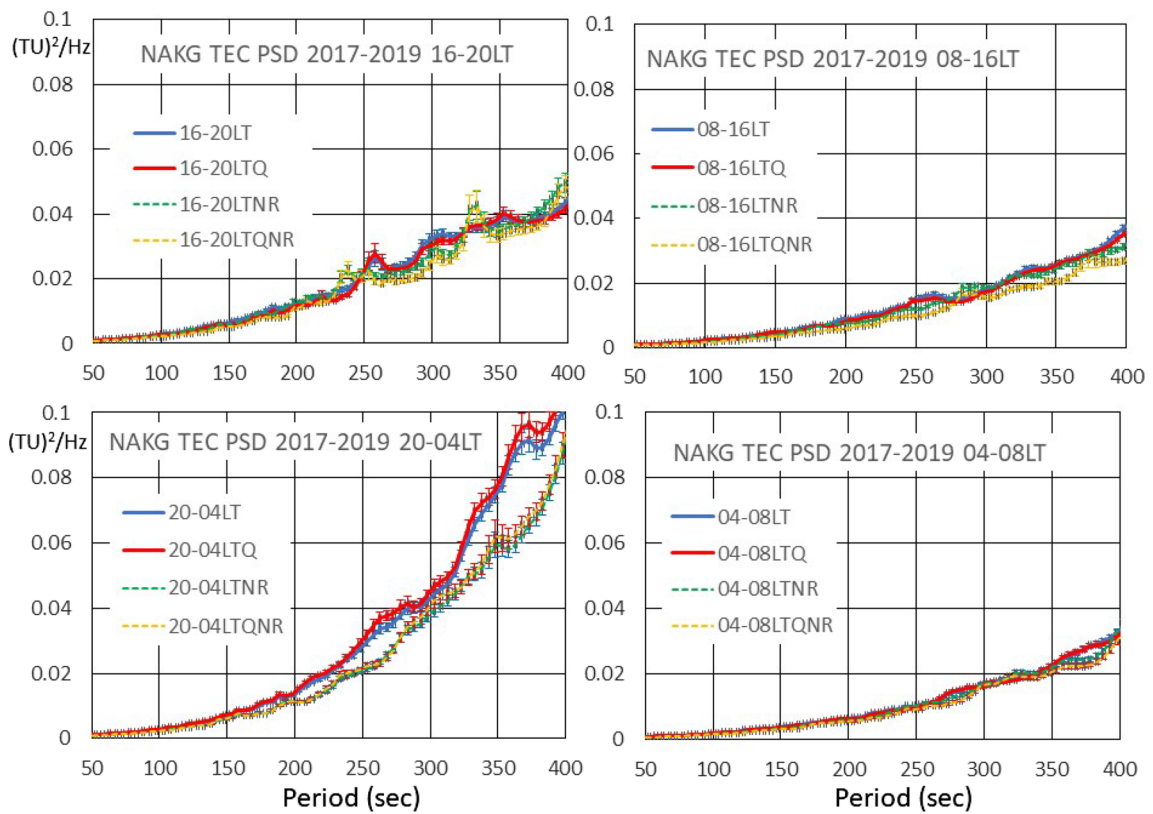


Fig. 12 Similar plots with Figs. 8 and 9 (but presented in one frame) for the PSD at Tokara Nakanoshima (NAKG) station, Japan

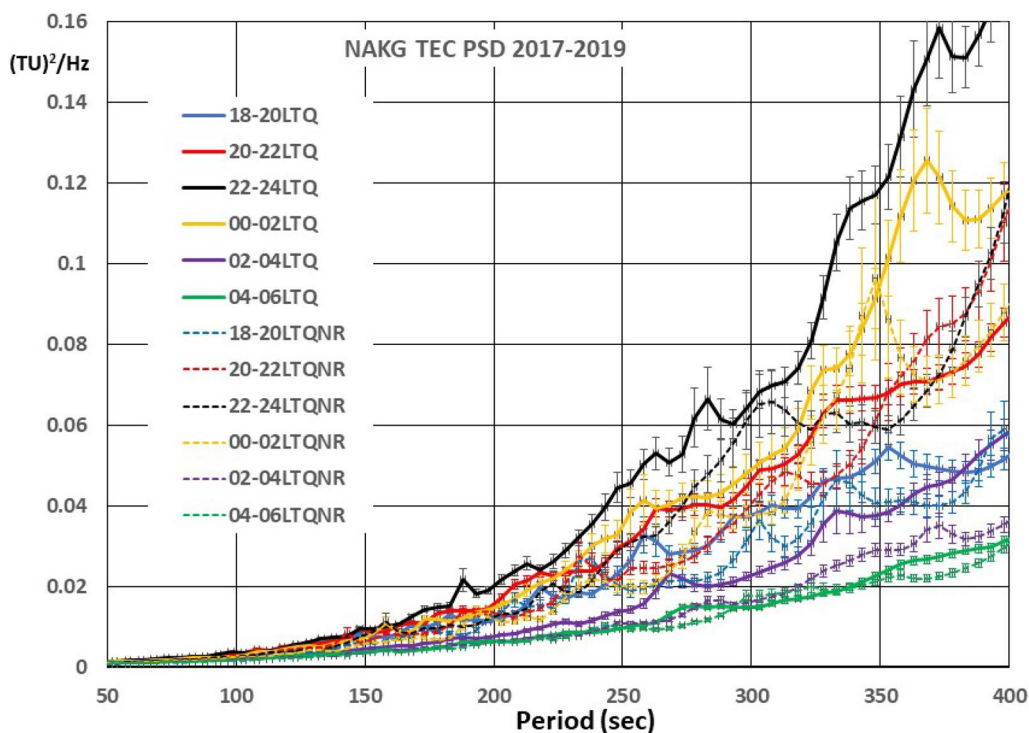


Fig. 13 A PSD plot for the TEC data from NAKG station. The local time is divided every 2 h for 18–06 LT zones similar to Fig. 10 to find the LT zone where the enhancement of the PSD in rainy condition is most clear. The difference between rainy cases and no-rain cases is most clear in 22–24LT zone. Thick lines are for the result in rainy condition (>0.08 mm/h) and thin broken lines are in almost no-rain (<0.002 mm/hour) condition

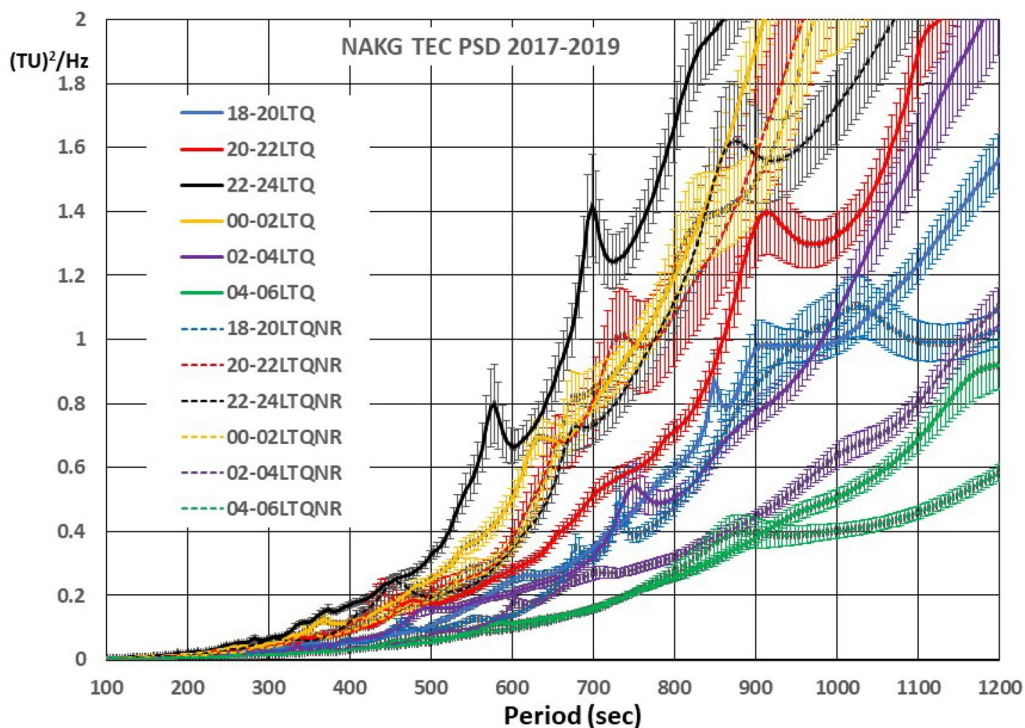


Fig. 14 Same as Fig. 13 but for wide range of period. In the LT zones of 22–24LT and 02–04LT, the PSD for rainy condition is larger than no-rain condition

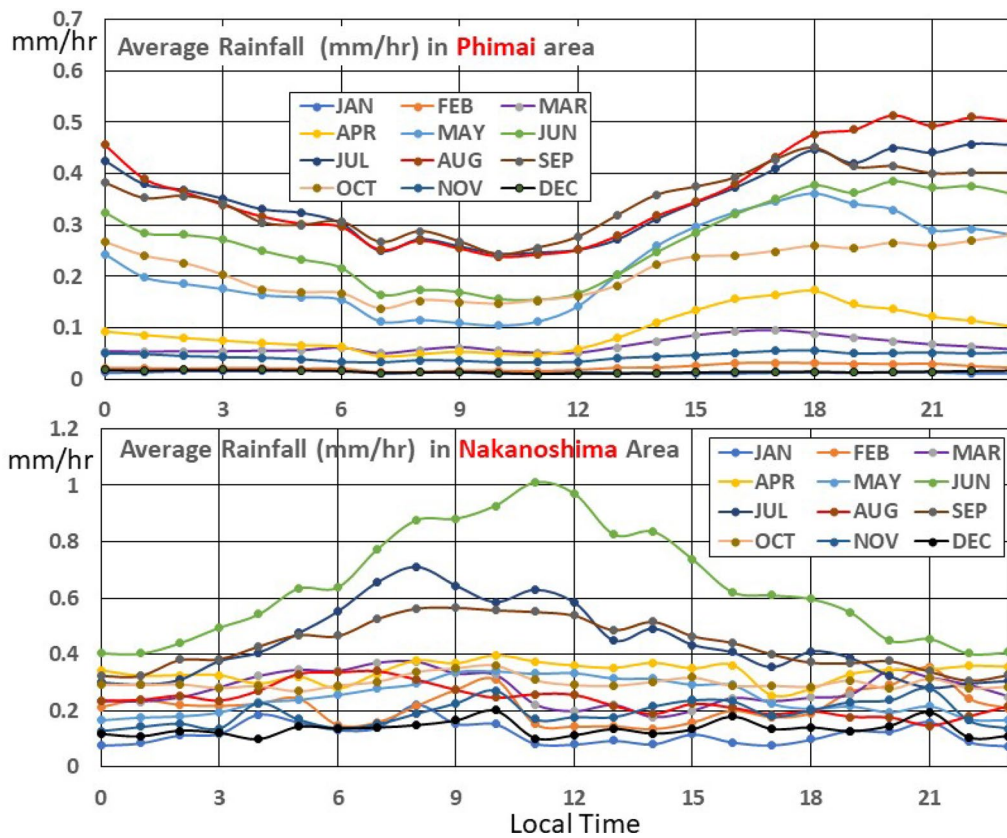


Fig. 15 Local time variation of average rainfall (mm/hour) in 720 × 720 km area surrounding the PHIM (upper panel) and the NAKG (lower panel) stations. Twelve lines with different color indicate 12 monthly averaged LT variations, respectively. The dot at Local time = 0 in this figure corresponds to an average for 00LT – 01LT period. The data period used for Phimai area is from March 2014 to December 2020, and that for Nakanoshima area is from July 2017 to July 2019. Period of no available GPS data is not included

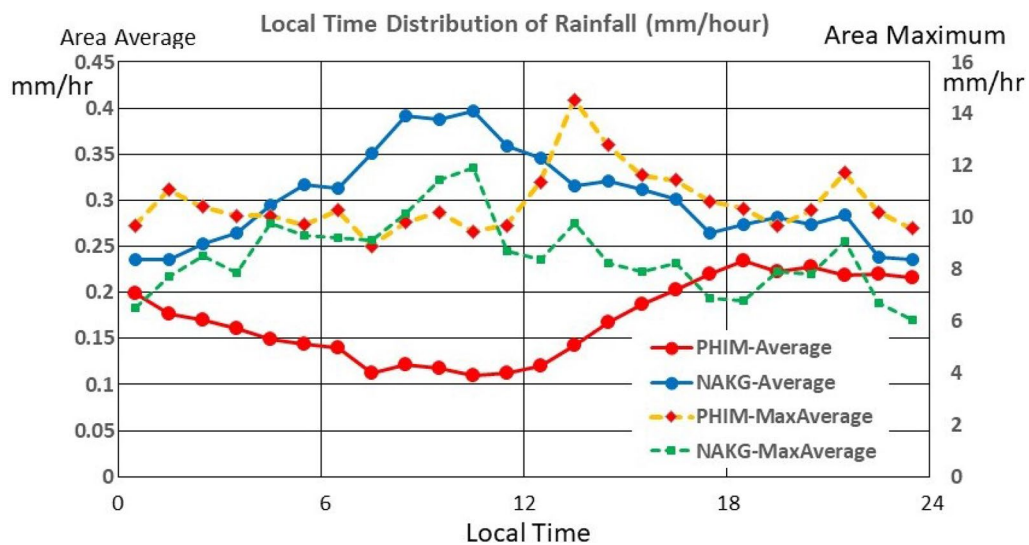


Fig. 16 Averaged precipitation in 720 × 720 km area surrounding the PHIM and NAKG stations. The data periods are the same with those used in Fig. 15. Both a simple average in the areas indicated by solid lines (scale is on the left side) and an average of maximum intensity among 0.1 × 0.1 mesh points indicated broken lines (scale is on the right side) are presented. In PHIM area, the average rainfall is maximum in the evening. On the other hand, the average of maximum intensity is at 14LT, i.e., in early afternoon

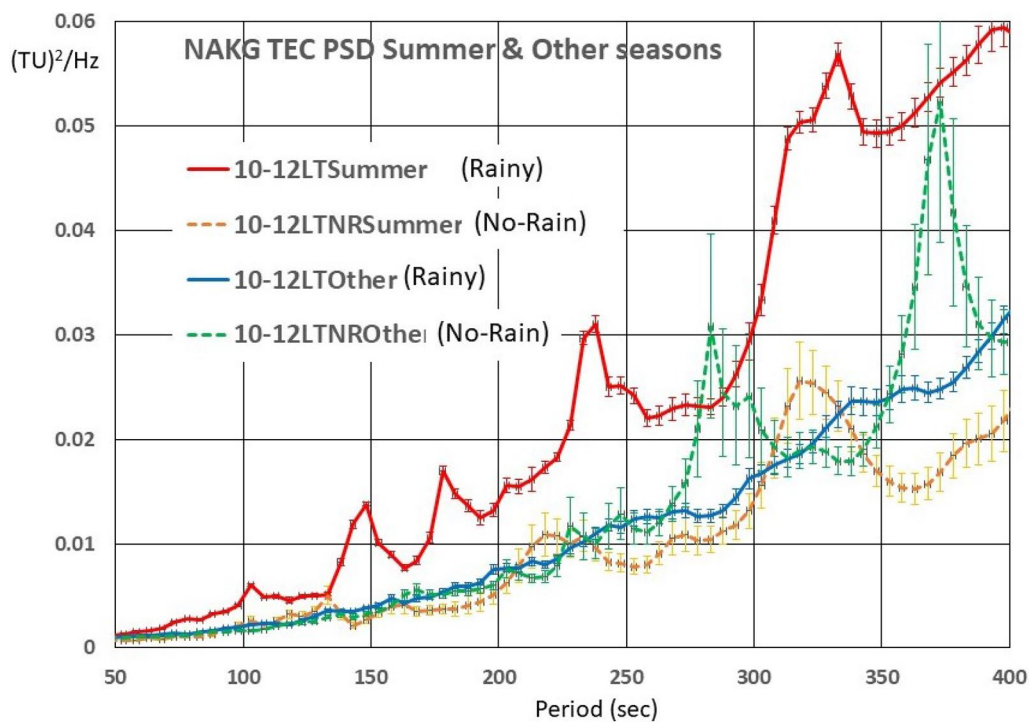


Fig. 17 A comparison of the results for summer season (Jun–Aug) and for other months at NAKG station. LT zone is 10–12LT when the average rainfall is largest in June. For this LT zone, a clear difference in the PSD of TEC variation between rainy condition and no-rain condition appears in summer (red and orange lines, respectively). On the other hand, no clear difference appears in other seasons (blue and green lines)

GSMaP data suggest that a localized heavy rain such as the rainfall in tropical squall tends to occur in the afternoon. This suggests that the LT difference of TEC PSD could come from both the LT dependence of rainfall and the difference in the type of rainfall. The NAKG data also suggest the amount of average rainfall to be an important factor. To check this point, we may need not only to use the average rainfall, but also to categorize the type of rainfall, i.e., rainfall in wide area or localized heavy rainfall, continuous or variable in short time scale, etc.

Another possibility of evening-side enhancement could be the effect of sharp electron density gradient after sunset. That is, the equatorial fountain effect causes dense F-region during the daytime, and a sharp density gradient after the sunset is expected to develop.

Then a small fluctuation of electron density caused by the atmospheric waves generated in rainy condition could be amplified by a plasma instability such as Rayleigh–Taylor instability.

At the PHIM station, a clear bulge around 275 s appears in the average PSD on the dusk side. This suggests the contribution of vertical acoustic resonance caused by the strong rainfall or associated cumulus convection in tropical zone. Although the peak frequency is often slightly different from the well-known major resonance frequencies, an example on April 25, 2014 (Fig. 19) or another on March 18, 2017 (Fig. 4) also suggests a resonance effect to the enhancement of the TEC fluctuations. The complexity shown in Fig. 20 (left panel) may partly come from such resonance-like effects locally develop over the area of active cumulus convection.

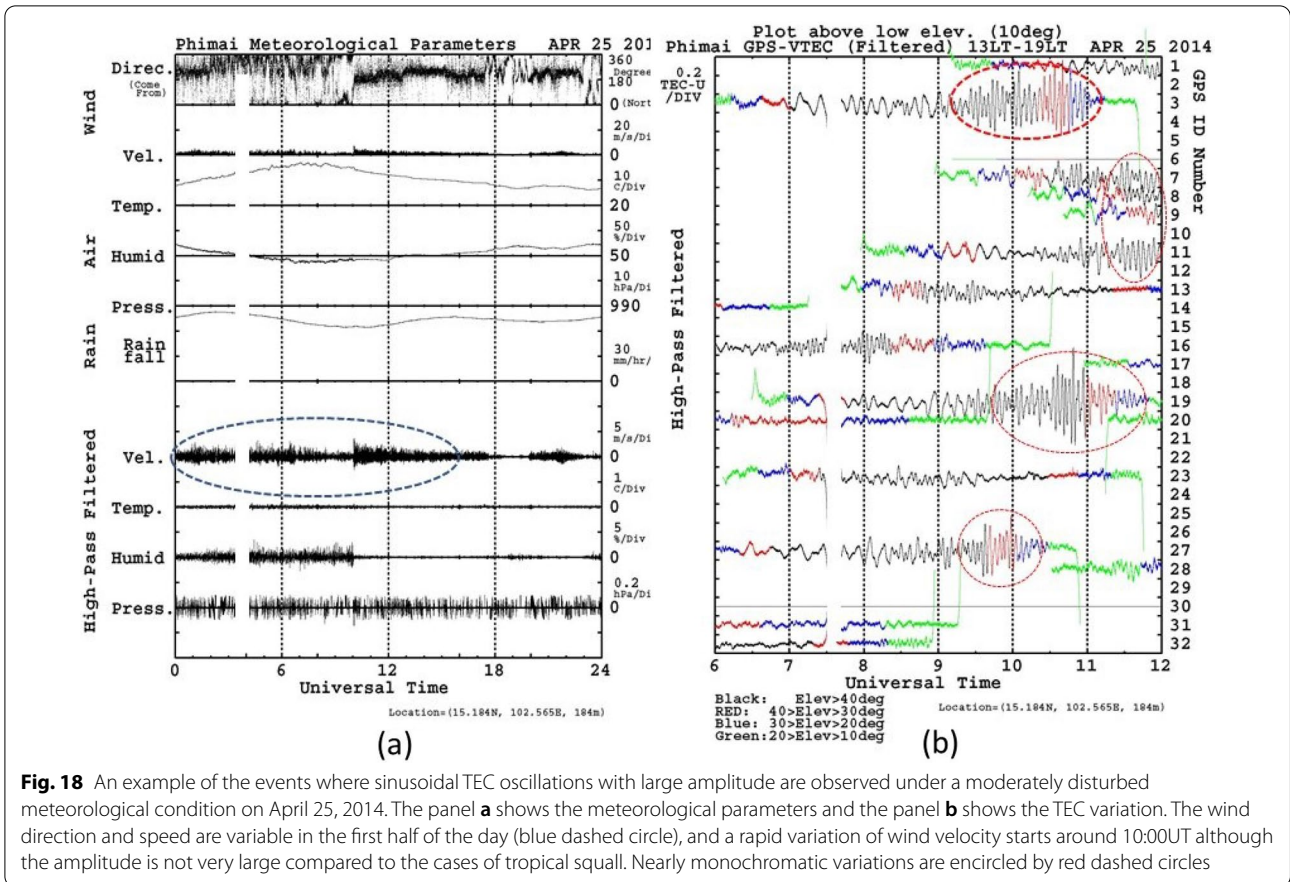


Fig. 18 An example of the events where sinusoidal TEC oscillations with large amplitude are observed under a moderately disturbed meteorological condition on April 25, 2014. The panel **a** shows the meteorological parameters and the panel **b** shows the TEC variation. The wind direction and speed are variable in the first half of the day (blue dashed circle), and a rapid variation of wind velocity starts around 10:00UT although the amplitude is not very large compared to the cases of tropical squall. Nearly monochromatic variations are encircled by red dashed circles

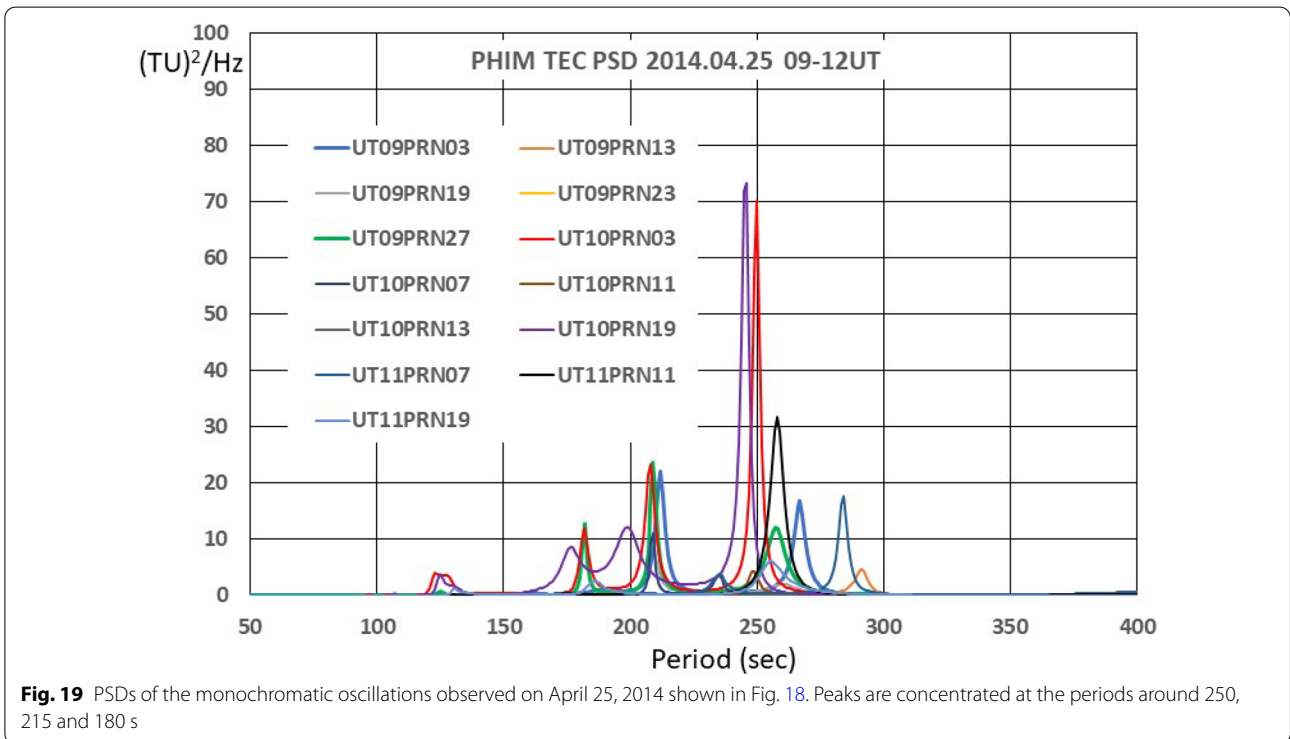
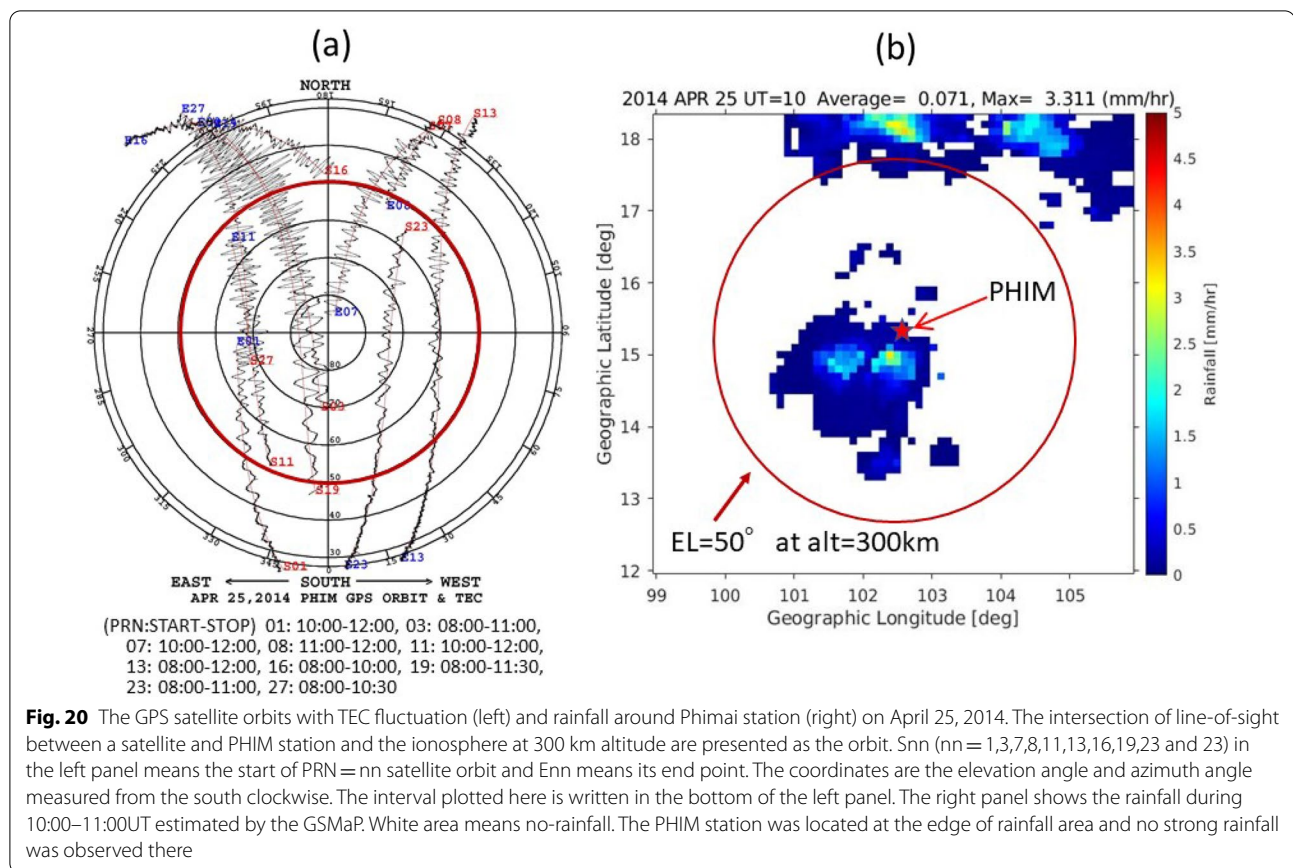


Fig. 19 PSDs of the monochromatic oscillations observed on April 25, 2014 shown in Fig. 18. Peaks are concentrated at the periods around 250, 215 and 180 s



Abbreviations

EL: Elevation angle; GPS: Global Positioning System; GSMaP: Global satellite mapping of precipitation; JAXA: Japan Aerospace Exploration Agency; JSPS: Japan Society for the Promotion of Science; LT: Local time; MEM: Maximum entropy method; PSD: Power spectral density; TEC: Total electron content; UT: Universal time.

Acknowledgements

We thank Profs. Michio Hashizume, Teruyuki Nakajima, Yoshikazu Tanaka, Manabu Hashimoto, Masahito Nose and Niithiwatthn Choosakul for their contribution in opening the Phimai Atmospheric Observatory and installing various instruments. We thank Prof. Shinichi Miyazaki and Dr. Takuji Kazama for providing a GPS receiver for observation at PHIM station. We also thank many other staff and students at the Chulalongkorn University, Kyoto University, JAMSTEC, Chiba University and Ibaraki University for their help to continue observation at Phimai, Thailand, and at Tokara Nakanoshima Island, Japan. We also thank JAXA/GSMaP project team for providing the global precipitation data. This study has been supported by the JSPS grants 15H05815, 17K05669, 20H00099 and 21K03643. The authors thank the World Data Center for Geomagnetism, Kyoto, for keeping the data used in this paper.

Authors' contributions

TI, YS, YO and YY installed weather stations, magnetometers and barometers at Phimai and Nakanoshima stations and operated them. AY and TA made preparative studies on the relation between rainfall and GPS-TEC or satellite magnetic observations. KH and AS installed a GPS receiver at Phimai and derived the TEC. VP and TJ maintained the observation at Phimai. MI made the GPS observation at NAKG station. TI conducted this research and mainly processed and analyzed the data. All authors read and approved the final manuscript.

Funding

This study has been supported by the JSPS grants (Kakenhi) 15H05815, 17K05669, 20H00099 and 21K03643.

Availability of data and materials

Information on the GSMaP data and their use are obtained from <https://shara.ku.eorc.jaxa.jp/GSMaP/guide.html>. Registration is requested to download by ftp. The Kp index is available from <https://www.gfz-potsdam.de/en/kp-index/>. The GPS-TEC and weather station data obtained at the Phimai and Nakanoshima Is. are available on request base.

Declarations

Ethics approval and consent to participate

Not applicable.

Consent for publication

Not applicable.

Competing interests

The authors declare that they have no competing interests.

Author details

¹Graduate School of Science, Kyoto University, Kita-shirakawa Oiwake-cho, Sakyo-ku, Kyoto 606-8502, Japan. ²F-Factory Co., Ltd., Kasugaoka 1-129, Nabari 518-0453, Japan. ³National Institute of Information and Communications Technology, Nukui Kita-machi, Koganei 184-8795, Japan. ⁴Swedish Institute of Space Physics, Box 812, 981 28 Kiruna, Sweden. ⁵Asahi University,

Hozumi 1851, Mizuho 501-0296, Japan. ⁶Faculty of Science, Chulalongkorn University, 254 Phayathai Road, Bangkok 10330, Thailand. ⁷Disaster Prevention Institute, Kyoto University, Uji 611-0011, Japan.

Received: 18 January 2022 Accepted: 7 March 2022
Published online: 02 April 2022

References

- Aoyama T, Iyemori T, Nakanishi K, Nishioka M, Rosales D, Veliz O, Safor EV (2016) Localized field-aligned currents and 4-min TEC and ground magnetic oscillations during the 2015 eruption of Chile's Calbuco volcano. *Earth Planet Sp* 68(1):148. <https://doi.org/10.1186/s40623-016-0523-0>
- Aoyama T, Iyemori T, Nakanishi K (2017) Magnetic ripples observed by Swarm satellites and their enhancement during typhoon activity. *Earth Planet Sp* 69:89. <https://doi.org/10.1186/s40623-017-0679-2>
- Calais E, Minster JB (1995) GPS detection of ionospheric perturbations following the January 17, 1994, Northridge earthquake. *Geophys Res Lett* 22:1045–1048. <https://doi.org/10.1029/95GL00168>
- Choosakul N, Saito A, Iyemori T, Hashizume M (2009) Excitation of 4-min periodic ionospheric variations following the great Sumatra-Andaman earthquake in 2004. *J Geophys Res* 114:A10313. <https://doi.org/10.1029/2008JA013915>
- Heki K, Ping J (2005) Directivity and apparent velocity of coseismic ionospheric disturbances observed with a dense GPS array. *Earth Planet Sci Lett* 236:845–855. <https://doi.org/10.1016/j.epsl.2005.06.010>
- Heki K, Sugawara M, Ozeki M, Okazaki I (2010) Geophysics with GPS-TEC. *J Geod Soc Japan* 56:125–134 (in Japanese)
- Iyemori T, Nosé M, Han D-S, Gao Y, Hashizume M, Choosakul N, Shinagawa H, Tanaka Y, Utsugi M, Saito A, McCreddie H, Odagi Y, Yang F (2005) Geomagnetic pulsations caused by the Sumatra earthquake on December 26, 2004. *Geophys Res Lett* 32:L20807. <https://doi.org/10.1029/2005GL024083>
- Iyemori T, Aoyama T, Yokoyama Y (2022) Global distribution of magnetic ripples and electron density fluctuations as observed by the Swarm satellites on the dayside and their relation to the rainfall estimated by the GSMaP. *Earth Planet Sp* 74:38. <https://doi.org/10.1186/s40623-022-01597-3>
- Kanamori H, Mori J, Harkrider DG (1994) Excitation of atmospheric oscillations by volcanic eruptions. *J Geophys Res* 99:21947–21961. <https://doi.org/10.1029/94JB01475>
- Nakanishi K, Iyemori T, Taira K, Lühr H (2014) Global and frequent appearance of small spatial scale field aligned currents possibly driven by the lower atmospheric phenomena as observed by the CHAMP satellite in middle and low latitudes. *Earth Planet Sp* 66:40. <https://doi.org/10.1186/1880-5981-66-40>
- Nishioka M, Tsugawa T, Kubota M, Ishii M (2013) Concentric waves and short-period oscillations observed in the ionosphere after the 2013 Moore EF5 tornado. *Geophys Res Lett*. <https://doi.org/10.1002/2013GL057963>
- Saito A, Tsugawa T, Otsuka Y, Nishioka M, Iyemori T, Matsumura M, Saito S, Chen CH, Goi Y, Choosakul N (2011) Acoustic resonance and plasma depletion detected by GPS total electron content observation after the 2011 Tohoku Earthquake. *Earth Planet Sp* 63:863–867. <https://doi.org/10.5047/eps.2011.06.034>
- Shinagawa H, Iyemori T, Saito S, Maruyama T (2007) A numerical simulation of ionospheric and atmospheric variations associated with the Sumatra earthquake on December 26, 2004. *Earth Planet Sp* 59:1015–1026. <https://doi.org/10.1186/BF03352042>
- Zettergren MD, Snively JB (2015) Ionospheric response to infrasonic-acoustic waves generated by natural hazard events. *J. Geophys Res Sp Phys* 120:8002–8024. <https://doi.org/10.1002/2015JA021116>

Publisher's Note

Springer Nature remains neutral with regard to jurisdictional claims in published maps and institutional affiliations.

Submit your manuscript to a SpringerOpen[®] journal and benefit from:

- Convenient online submission
- Rigorous peer review
- Open access: articles freely available online
- High visibility within the field
- Retaining the copyright to your article

Submit your next manuscript at ► [springeropen.com](https://www.springeropen.com)